

## 1           **The Pathogenicity of 2019 Novel Coronavirus in hACE2 Transgenic Mice**

2

3   Linlin Bao<sup>†1</sup>, Wei Deng<sup>†1</sup>, Baoying Huang<sup>†2</sup>, Hong Gao<sup>†1</sup>, Lili Ren<sup>3</sup>, Qiang Wei<sup>1</sup>, Pin  
4   Yu<sup>1</sup>, Yanfeng Xu<sup>1</sup>, Jiangning Liu<sup>1</sup>, Feifei Qi<sup>1</sup>, Yajin Qu<sup>1</sup>, Wenling Wang<sup>2</sup>, Fengdi Li<sup>1</sup>, Qi  
5   Lv<sup>1</sup>, Jing Xue<sup>1</sup>, Shuran Gong<sup>1</sup>, Mingya Liu<sup>1</sup>, Guanpeng Wang<sup>1</sup>, Shunyi Wang<sup>1</sup>, Linna  
6   Zhao<sup>1</sup>, Peipei Liu<sup>2</sup>, Li Zhao<sup>2</sup>, Fei Ye<sup>2</sup>, Huijuan Wang<sup>2</sup>, Weimin Zhou<sup>2</sup>, Na Zhu<sup>2</sup>, Wei Zhen<sup>2</sup>,  
7   Xiaojuan Zhang<sup>2</sup>, Zhiqi Song<sup>1</sup>, Li Guo<sup>3</sup>, Lan Chen<sup>3</sup>, Conghui Wang<sup>3</sup>, Ying Wang<sup>3</sup>,  
8   Xinming Wang<sup>3</sup>, Yan Xiao<sup>3</sup>, Qiangming Sun<sup>4</sup>, Hongqi Liu<sup>4</sup>, Fanli Zhu<sup>4</sup>, Chunxia Ma<sup>4</sup>,  
9   Lingmei Yan<sup>4</sup>, Mengli Yang<sup>4</sup>, Jun Han<sup>2</sup>, Wenbo Xu<sup>2</sup>, Wenjie Tan<sup>2</sup>, Xiaozhong Peng<sup>4</sup>, Qi  
10   Jin<sup>3</sup>, Guizhen Wu<sup>\*2</sup>, Chuan Qin<sup>\*1</sup>

11

12   <sup>1</sup> Key Laboratory of Human Disease Comparative Medicine, Chinese Ministry of Health,  
13   Beijing Key Laboratory for Animal Models of Emerging and Reemerging Infectious  
14   Diseases, Institute of Laboratory Animal Science, Chinese Academy of Medical Sciences  
15   and Comparative Medicine Center, Peking Union Medical College, Beijing, China.

16   <sup>2</sup> MHC Key Laboratory of Biosafety, National Institute for Viral Disease Control and  
17   Prevention, China CDC, Beijing, China.

18   <sup>3</sup> Institute of Pathogen Biology, Chinese Academy of Medical Sciences, Beijing, China.

19   <sup>4</sup> Institute of Medical Biology, Chinese Academy of Medical Sciences, Beijing, China.

20

21   <sup>†</sup>These authors contributed equally to this work.

22   \*Correspondence should be addressed to Chuan Qin, Email: [qinchuan@pumc.edu.cn](mailto:qinchuan@pumc.edu.cn), or

23   Guizhen Wu, Email: [wugz@ivdc.chinacdc.cn](mailto:wugz@ivdc.chinacdc.cn).

24 **Abstract**

25 2019-nCoV caused pneumonia cases in China has become a public health emergency of  
26 international concern (PHEIC). The first priority for prevention and treatment of the  
27 disease is to find the pathogenicity of 2019-nCoV *in vivo*. Weight loss and virus replication  
28 were detected in infected-hACE2 mice. The typical histopathology was interstitial  
29 pneumonia with significant inflammatory cells infiltration around the bronchioles and  
30 blood vessels, and viral antigens were observed in bronchial epithelial cells and alveolar  
31 epithelial cells. The phenomenon was not found in wild type mice infected with 2019-  
32 nCoV and the mock-infected hACE2 mice. The pathogenicity of 2019-nCoV in hACE2  
33 mice was clarified and the Koch's postulates was fulfilled as well, and the model may  
34 facilitate the development of therapeutics and vaccines against 2019-nCoV.

35

36 In late December of 2019, a cluster of severe pneumonia cases caused by 2019 novel  
37 coronavirus (2019-nCoV), linked to a seafood market in which exotic animals were also  
38 sold and consumed, were identified and reported from Wuhan City, Hubei Province,  
39 China<sup>1,2</sup>. The number of infections has since soared, with almost 10,000 cases reported and  
40 over 200 deaths as of January 31, 2020 in China<sup>3</sup>, and imported cases from travelers of  
41 mainland China in several other countries. It is critical to find the pathogenicity and biology  
42 of the virus for prevention and treatment of the disease.

43 Because 2019-nCoV was highly homologous with Severe acute respiratory syndrome  
44 coronavirus (SARS-CoV), human Angiotensin-converting enzyme 2 (hACE2), which was  
45 the entry receptor of SARS-CoV, was also considered to have a high binding ability with  
46 the 2019-nCoV by molecular biological analysis<sup>4,5</sup>. Therefore, we used the hACE2  
47 transgenic and wild type mice infected with or without 2019-nCoV infection to study the  
48 pathogenicity of the virus. Specific pathogen-free, 6-11-month-old, male and female  
49 hACE2 mice and wild type mice (n=7) were inoculated intranasally with 2019-nCoV stock  
50 virus at a dosage of  $10^5$  TCID<sub>50</sub> per mouse, and the mock-infected hACE2 mice (n=3) were  
51 used as control. Weight loss of up to 5% was observed for 10 dpi only in the 2019-nCoV-  
52 infected hACE2 mice (Figure 1a), and other clinical symptoms were not observed. Major  
53 organs were harvested at 3 dpi and 5 dpi to assess for biodistribution of 2019-nCoV in  
54 infected hACE2 mice. Viral RNA was positive by RT-PCR (Figure 1b) and identified by  
55 sequencing only in the lung of infected-hACE2 mice at 3 dpi and 5 dpi. Meanwhile, the  
56 virus was successfully isolated by Vero cells culture (Figure 1d) and observed by an  
57 electron microscope (Figure 1e). However, the virus was not found in the PBS-infected  
58 hACE2 mice or infected-wild type mice (data not shown).

59           The typical pneumonia was demonstrated as bilateral ground-glass opacity and  
60 subsegmental areas of consolidation by image in patient<sup>6</sup>, but no histopathological results  
61 were reported until now. The major organs of mice were examined by histopathology and  
62 immunofluorescence. Compared to PBS-infected hACE2 mice or 2019-nCoV-infected-  
63 wild type mice (Figure 2a and b), focal lesions were observed in the dorsal of the right  
64 middle lobe in 2019-nCoV-infected hACE2 mice (Figure 2c). Consistently, lung tissues  
65 from 2019-nCoV-infected hACE2 mice had multifocally mild or moderate pneumonia with  
66 interstitial hyperplasia. And significant inflammatory cells infiltration around the  
67 bronchioles and blood vessels (Figure 2f) were found. The alveolar interstitium is also  
68 expanded with inflammatory cells, and the alveolar lumen contains cell debris mixed with  
69 leukocytes. Bronchial epithelial cells showed swelling, degeneration, and some of them  
70 dissolved and necrotic foci (Figure 2g, h and i). Meanwhile, 2019-nCoV antigens were  
71 observed in the bronchial epithelial cells (Figures 3h and i) and alveolar epithelial cells  
72 (Figures 3n, o, p and q) of lungs in 2019-nCoV-infected hACE2 mice. In addition, the co-  
73 localization of 2019-nCoV S protein and hACE2 receptor was demonstrated in alveolar  
74 epithelial cells of infected-hACE2 mice by immunofluorescence (Figures 3n, o, p and q).  
75 The phenomenon was not found in the PBS-infected hACE2 mice (Figures 3k, i and m) or  
76 infected-wild type mice (data not shown).

77           The speed of geographical spread of severe viral pneumonia disease caused by 2019-  
78 nCoV has been declared as public health emergency of international concern (PHEIC),  
79 with cases reported on multiple continents only weeks after the disease was first reported<sup>7</sup>.  
80 Although it has been determined by bioinformatics that the pathogen of this epidemic is a  
81 novel coronavirus, it is necessary to be confirmed by animal experiments following Koch's

82 principles. After experimental infection of transgenic hACE2 mice with one of the earliest  
83 known isolates of 2019-nCoV, the mice lost weight and showed interstitial pneumonia,  
84 which are comparable with initial clinical reports of pneumonia caused by 2019-nCoV<sup>6</sup>.  
85 In addition, the 2019-nCoV S protein and hACE2 receptor were found to co-localize in  
86 alveolar epithelial cells, supporting that the 2019-nCoV, similar to SARS-CoV, also  
87 utilizes the hACE2 as a receptor for entry<sup>4</sup>. Therefore, the present study clarified the  
88 pathogenicity of 2019-nCoV in hACE2 mice and fulfills the Koch's postulates as well, and  
89 the model may facilitate the development of drugs and vaccines against 2019-nCoV.

90

## 91 **Materials and methods**

### 92 *Ethics statement*

93 Murine studies were performed in an animal biosafety level 3 (ABSL3) facility using  
94 HEPA-filtered isolators. All procedures in this study involving animals were reviewed and  
95 approved by the Institutional Animal Care and Use Committee of the Institute of  
96 Laboratory Animal Science, Peking Union Medical College (BLL20001).

97

### 98 *Viruses and cells*

99 The 2019-nCoV (strain HB-01) was kindly provided by Professor Wenjie Tan<sup>1</sup>, from the  
100 China Centers for Disease Control and Prevention (China CDC). The complete genome for  
101 this 2019-nCoV was submitted to GISAID (BetaCoV/Wuhan/IVDC-HB-  
102 01/2020|EPI\_ISL\_402119), and deposited in the China National Microbiological Data  
103 Center (accession number NMDC10013001 and genome accession numbers  
104 MDC60013002-01). Seed 2019-nCoV stocks and virus isolation studies were performed

105 in Vero cells, which are maintained in Dulbecco's modified Eagle's medium (DMEM,  
106 Invitrogen, Carlsbad, USA) supplemented with 10% fetal bovine serum (FBS), 100 IU/ml  
107 penicillin, and 100 µg/ml streptomycin, and incubated at 37°C, 5% CO<sub>2</sub>. Titers for 2019-  
108 nCoV were determined using a standard 50% tissue culture infection dose (TCID<sub>50</sub>) assay.

109

### 110 *Animal experiments*

111 For the animal experiments, specific pathogen-free, 6-11-month-old, male and female  
112 transgenic hACE2 mice were obtained from the Institute of Laboratory Animal Science,  
113 Peking Union Medical College, China. Transgenic mice were generated by microinjection  
114 of the mice hACE2 promoter driving the human ACE2 coding sequence into Institute of  
115 Cancer Research (ICR) or C57BL/6J mice; the presence of human ACE2 in the mice used  
116 for these experiments was confirmed by PCR (data not shown). The hACE2 mice (n=7)  
117 or ICR mice (n=5) were respectively inoculated intranasally with 2019-nCoV stock virus  
118 at a dosage of 10<sup>5</sup> TCID<sub>50</sub> per mouse. As a control, hACE2 mice (n=3) were mock-infected  
119 with an equivalent challenge volume of PBS. PBS- and 2019-nCoV-infected animals were  
120 continuously observed daily to record body weights, clinical symptoms, decreased  
121 responsiveness to external stimuli and death. Two mice from the 2019-nCoV-infected  
122 group were dissected at 3 days post-infection (dpi) and at 5 dpi to collect trachea, lung,  
123 kidney, brain, spleen, and liver tissues for the determination of viral load after 2019-nCoV  
124 infection. One mouse from the PBS-infected group was dissected at 3 dpi as a control. One  
125 mouse from the ICR mice group inoculated with 2019-nCoV was dissected at 3 dpi as the  
126 receptor control.

127

128 *Preparation of Homogenate Supernatant*

129 Tissues homogenates were prepared by homogenizing perfused whole tissue using an  
130 electric homogenizer for 2 min 30 s in 1 ml of DMEM. The homogenates were centrifuged  
131 at 3,000 rpm for 10 min at 4°C. The supernatant was collected and stored at -80°C for viral  
132 isolation and viral load detection.

133

134 *RNA extraction and RT-PCR*

135 Total RNA was extracted from organs using the RNeasy Mini Kit (Qiagen, Hilden,  
136 Germany), and reverse transcription was performed using the PrimerScript RT Reagent Kit  
137 (TaKaRa, Japan) following manufacturer instructions. RT-PCR reactions were performed  
138 using the PowerUp SYBG Green Master Mix Kit (Applied Biosystems, USA), in which  
139 samples were processed in duplicate using the following cycling protocol: 50°C for 30 min,  
140 95°C for 15 min, followed by 40 cycles at 94°C for 15 s and 60°C for 45 s. The primer  
141 sequences used for RT-PCR are targeted against the envelope (E) gene of 2019-nCoV and  
142 are as follows: Forward: 5'-TCAGAATGCCAATCTCCCAAC-3', Reverse: 5'-  
143 AAAGGTCCACCCGATACATTGA-3'.

144

145 *Laboratory preparation of the antibody of 2019-nCoV Spike-1 (S1) protein*

146 Mice were immunized with purified 2019-nCoV S1 protein (Sino biological) and  
147 splenocytes of hyper immunized mice were fused with myeloma cells. Positive clones were  
148 selected by ELISA using 2019-nCoV S1 protein (Supplementary Figure 1). The cell  
149 supernatant of 7D2 clone, binding to 2019-nCoV S1 protein, was collected for  
150 immunofluorescence analysis.

151

152 *Hematoxylin and Eosin Staining*

153 For each mouse, the whole left lung was embedded in Cryo-Gel for histological  
154 examination by frozen section method. The lung tissue sections (10  $\mu$ m) were fixed in 100%  
155 acetone for 15 minutes and stained with Hematoxylin and Eosin (H&E). The  
156 histopathology of the lung tissue was observed by light microscopy.

157

158 *Immunofluorescence and confocal microscopy*

159 For viruses and ACE2 receptor localization analysis, the lung tissue sections (10  $\mu$ m) were  
160 washed twice with PBS, fixed by Immunol Staining Fix Solution (P0098), blocked 1 hour  
161 at room temperature by Immunol Staining Blocking Buffer (P0102) and then incubated  
162 overnight at 4°C with the appropriate primary and secondary antibodies. The nuclei were  
163 stained with DAPI. First, anti-2019-nCoV S protein (laboratory preparation) and sera of  
164 patient in convalescent phase were used to test the 2019-nCoV, respectively. Secondly, for  
165 analysis the relationship between 2019-nCoV and ACE2 receptor, anti-2019-nCoV S  
166 protein (mouse monoclonal 7D2, laboratory preparation, 1:200) and anti-hACE2 antibody  
167 (rabbit polyclonal, ab15348, Abcam1:200) were used. The sections was washed with PBS  
168 and incubated with secondary antibodies conjugated with FITC (goat anti-human, ab6854,  
169 Abcam, 1:200), TRITC (goat anti rabbit, ZF-0317, Beijing ZSGB Biotechnology, 1:200),  
170 or FITC (goat anti-mouse, ZF-0312, Beijing ZSGB Biotechnology, 1:200), respectively,  
171 dried at room temperature and observed via fluorescence microscopy.

172

173 *Statistical analysis*



174 All data were analyzed with GraphPad Prism 6.0 software. Statistically significant  
175 differences between the virus HB-01-infected hACE2 mice and other mice with or without  
176 HB-01 infection were determined using Welch's t-test. The level of statistical significance  
177 is designated as  $*p < 0.05$ ,  $**p < 0.01$  or  $\#p < 0.05$ ,  $\#\#p < 0.01$ .

178

## 179 **Acknowledgement**

180 We are grateful for Lianfeng Zhang and Xiuhong Yang to providing the hACE2 mice as a  
181 gift. We also thank Gary Wong for helping us proofread the language. This work was  
182 supported by the National Research and Development Project of China (Grant No.  
183 2020YFC0841100 and 2020YFC0842000), National Key Research and Development  
184 Project of China (Grant No. 2016YFD0500304), CAMS initiative for Innovative Medicine  
185 of China (Grant No. 2016-I2M-2-006), National Mega projects of China for Major  
186 Infectious Diseases (2017ZX10304402).

187

## 188 **References**

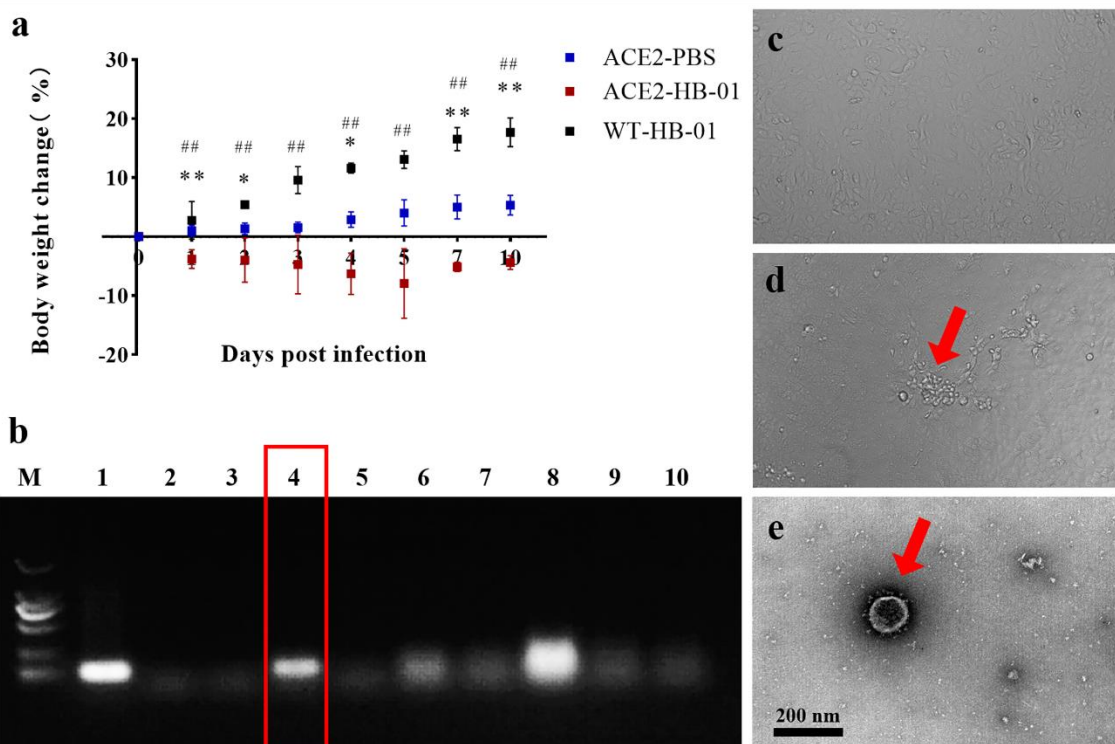
- 189 1. Zhu N, et al. A Novel Coronavirus from Patients with Pneumonia in China, 2019. *N Engl J Med*.  
190 2020 Jan 24. doi: 10.1056/NEJMoa2001017.
- 191 2. Ren LL, et al. Identification of a novel coronavirus causing severe pneumonia in human: a descriptive  
192 study. *Chin Med J (Engl)*. 2020 Jan 30. doi: 10.1097/CM9.0000000000000722.
- 193 3. China National Health Commission. Update on the novel coronavirus pneumonia outbreak (Jan 24,  
194 2020). Beijing: China National Health Commission, 2020.  
195 <http://www.nhc.gov.cn/yjb/s7860/202002/84faf71e096446fdb1ae44939ba5c528.shtml>.
- 196 4. Xintian Xu, et al. Evolution of the novel coronavirus from the ongoing Wuhan outbreak and modeling  
197 of its spike protein for risk of human transmission. *Science China*.2020.1.

198 5. Kuba K, et al. A crucial role of angiotensin converting enzyme 2 (hACE2) in SARS coronavirus-  
199 induced lung injury. *Nat Med.* 2005 Aug;11(8):875-9. doi: 10.1038/nm1267.

200 6. Huang C, et al. Clinical features of patients infected with 2019 novel coronavirus in Wuhan, China.  
201 *Lancet.* 2020 Jan 24. pii: S0140-6736(20)30183-5. doi: 10.1016/S0140-6736(20)30183-5.

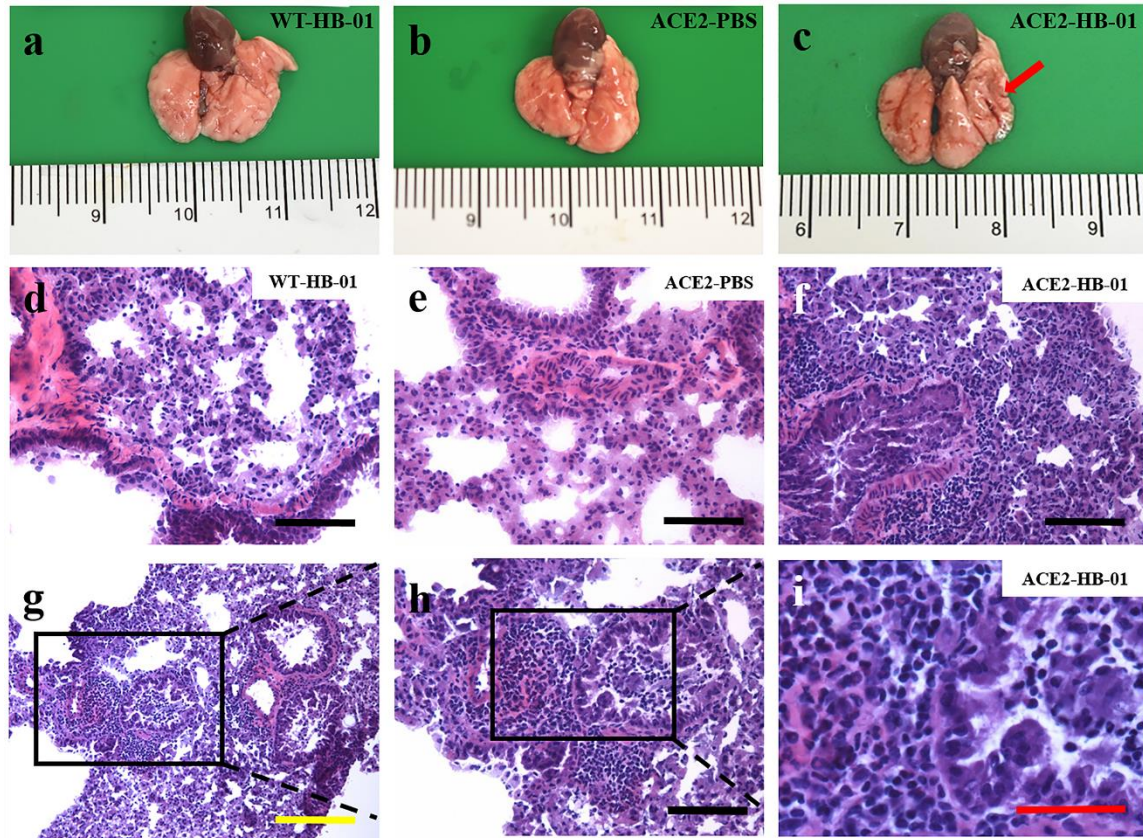
202 7. Chan JF, et al. A familial cluster of pneumonia associated with the 2019 novel coronavirus indicating  
203 person-to-person transmission: a study of a family cluster. *Lancet.* 2020 Jan 24. pii: S0140-  
204 6736(20)30154-9. doi: 10.1016/S0140-6736(20)30154-9.

205



206

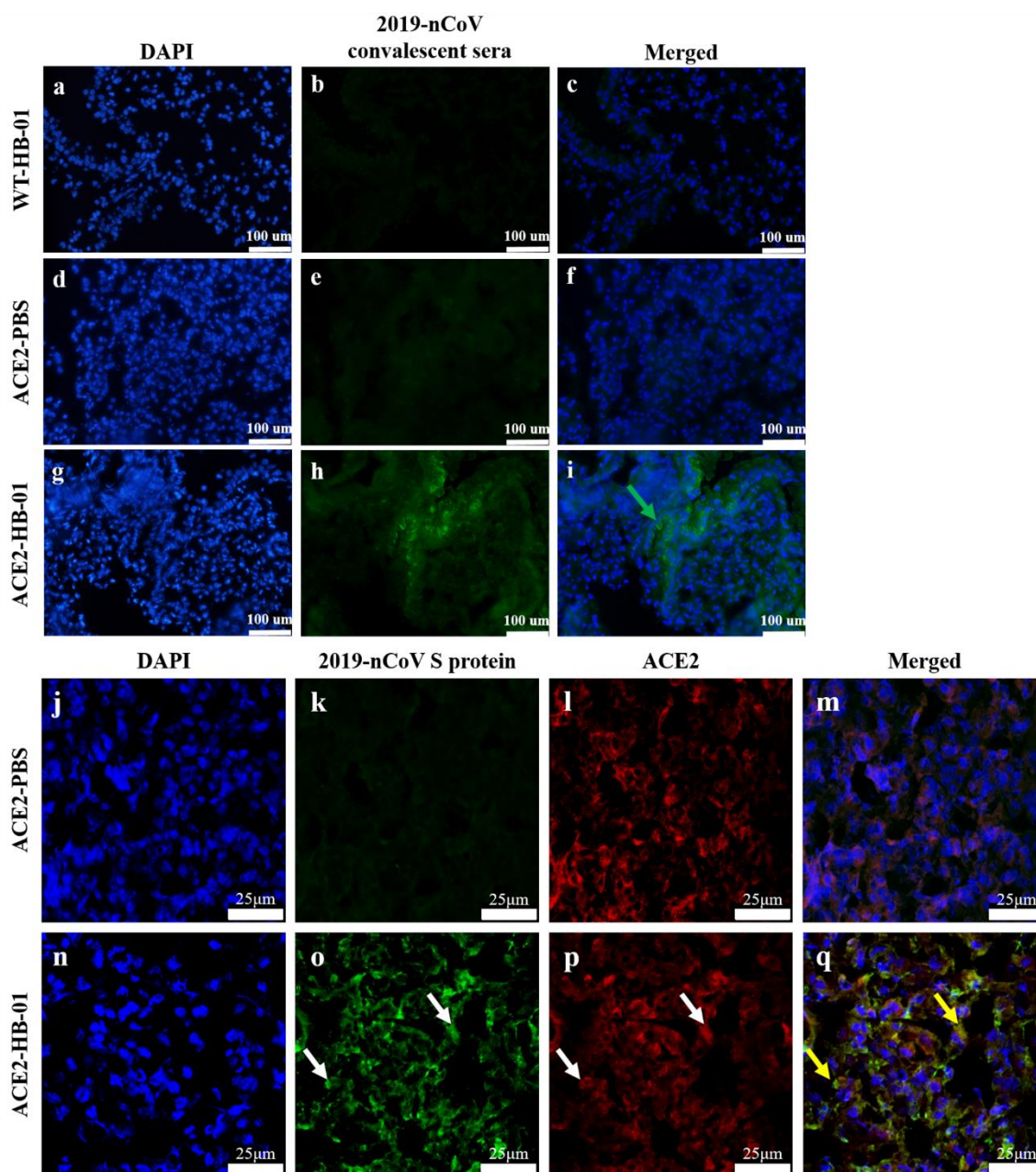
207 **Figure 1. Weight loss and virus detection in hACE2 mice post infection with 2019-**  
 208 **nCoV.** Two groups of mice were experimentally challenged intranasally with a dose of  $10^5$   
 209  $TCID_{50}$  2019-nCoV, and the PBS-infected hACE2 mice were used as control. WT mice  
 210 were inoculated with 2019-nCoV as receptor control. And then the weight loss was  
 211 recorded over 10 days (a). Mice were sacrificed and their major organs harvested for viral  
 212 load and virus isolation at 3 and 5 dpi, the distribution of 2019-nCoV in various organs of  
 213 infected hACE2 mice was detected by RT-PCR and the results of 3 dpi was  
 214 representatively shown (b) (line 1: positive control, line2: negative control, line 3-10:  
 215 trachea, lung, heart, spleen, intestine, liver, kidney and brain in turn). (c) Live virus could not be  
 216 isolated from the lungs of infected-WT mice on Vero cells, but (d) cytopathic effects were  
 217 observed from Vero cells infected with homogenate from the lungs of infected-hACE2  
 218 mice. Electron microscope pictures of 2019-nCoV from infected-hACE2 mice lung tissue  
 219 culture homogenate at 3 dpi (e). Significant differences are indicated with different  
 220 asterisks (Welch's t-test, ACE2-HB-01 vs ACE2-PBS,  $*p < 0.05$ ,  $**p < 0.01$ ; ACE2-HB-01  
 221 vs WT-HB-01,  $\#p < 0.05$ ,  $\#\#p < 0.01$ ).



222

223 **Figure 2. Gross pathology and histopathology of lungs of 2019-nCoV-infected hACE2**  
224 **mice.** Gross pathology of lungs from infected-WT mice (a), PBS-infected hACE2 mice (b)  
225 and 2019-nCoV-infected hACE2 mice (c) at 3 dpi. (d-i) Histological examination of lungs  
226 of infected-WT mice (d), PBS-infected hACE2 mice (e), and 2019-nCoV-infected hACE2  
227 mice (f-i). Histopathological examination of bronchioles and blood vessels (f) and alveolar  
228 interstitium (g-i) from infected-hACE2 mice. Yellow bar = 200  $\mu\text{m}$ , Black bar = 100  $\mu\text{m}$ ,  
229 Red bar = 50  $\mu\text{m}$ .

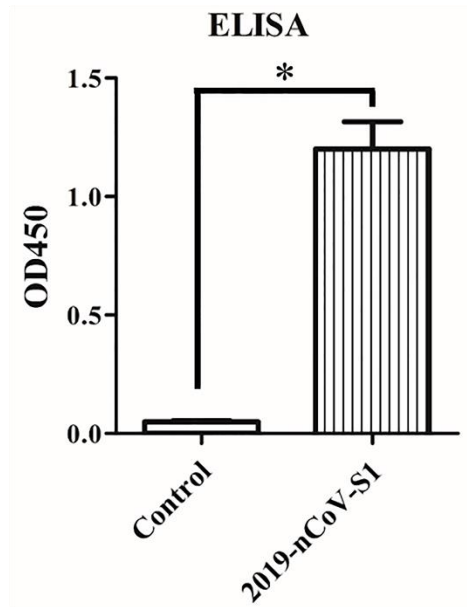
230



231

232 **Figure 3. Immunofluorescence analysis of viral antigens in lungs of 2019-nCoV-**  
233 **infected hACE2 mice.** (a-i): Fluorescence of sections of mice lungs after incubation with  
234 DAPI or antisera of 2019-nCoV-convalescent patients respectively. The lung sections of  
235 infected-WT mice (a-c), PBS-infected hACE2 mice (d-f) and infected-hACE2 mice (g-i).  
236 Green arrows indicate presence of 2019-nCoV in the alveolar epithelial cells. (j-q): Co-  
237 colocalization of 2019-nCoV S protein and hACE2 receptor in hACE2 mouse lungs, the  
238 sections were incubated with DAPI, a polyclonal antibody against 2019-nCoV S protein or

239 human ACE2 protein respectively. The lung sections of PBS-infected hACE2 mice (j-m).  
240 The lung sections of infected-hACE2 mice (n-q). The white arrows showed the viral S  
241 protein (o) and hACE2 (p) respectively, the yellow arrows showed the merge of viral S  
242 protein and hACE2 (q).  
243



244

245 **Supplementary Figure 1. Identification of 7D2 antibody against 2019-nCoV S1**  
246 **protein.** The plate coated by 0.2 ug 2019-nCoV S1 protein was incubated with 7D2  
247 antibody as primary antibody (1:200) and detected using HRP-conjugated goat anti-mouse  
248 secondary antibody. The titer of antibody was determined using enzyme-linked  
249 immunosorbent assay (ELISA) assay.

250